J. Am. Soc. Mass Spectrom. (2011) 22:2033–2041
DOI: 10.1007/s13361-011-0221-x

RESEARCH ARTICLE

Large Carbon Cluster Anions Generated by Laser Ablation of Graphene

Xianglei Kong,[1] Shuqi Li,[1] Sen Zhang,[1] Yi Huang,[2] Yongsheng Cheng[2]

[1]State Key Laboratory of Elemento-Organic Chemistry, Nankai University, Tianjin, China
[2]Key Laboratory of Functional Polymer Materials and Center for Nanoscale Science and Technology, Institute of Polymer Chemistry, College of Chemistry, Nankai University, Tianjin, China

Abstract

The formation of large even-numbered carbon cluster anions, C_n^-, with n up to 500 were observed in the mass spectra generated by laser ablation of graphene and graphene oxide, and the signal intensity of the latter is much weaker than that of the former. The cluster distributions generated from graphene can be readily altered by changing the laser energy and the accumulation period in the FT - ICR cell. By choosing suitable experimental conditions, weak signals of odd-numbered anions from C_{125}^- to C_{211}^-, doubly charged anions from C_{70}^{2-} to C_{230}^{2-} and triply charged cluster anions from C_{80}^{3-} to C_{224}^{3-} can be observed. Tandem MS was applied to some selected cluster anions. Though no fragment anions larger than C_{20}^- can be observed by the process of collisional activation with N_2 gas for most cluster ions, several cluster anions can lose units of C_2, C_4, C_6 or C_8 in their collision process. The differences in their dissociation kinetics and structures require further calculations and experimental studies.

Key words: Carbon cluster anion, Graphene, Laser ablation, CAD MS

Introduction

As one of the most amazing chemical elements, carbon is always telling us new and exciting stories. In addition to the traditional three-dimensional forms of diamond and graphite, the attention of scientific studies has been focusing on the zero-dimensional (fullerenes) and one-dimensional (nanotubes) forms for more than 20 years [1–5]. Recently, two-dimensional graphene has stimulated intense research interest due to its unique characteristics, including its band structure, massless fermions, and other features since it was first prepared by Novoselov et al. with a simple approach [6–11].

It is well known that mass spectrometry (MS) was critical to the discovery of the fullerenes [1–3, 12]. Nowadays, the rapid development of both fields of carbon materials and mass spectrometry allows them to be mutually beneficial. For example, it has been found that both nanodiamond and graphene have high affinities for biopolymers and can be used to enrich biomolecules in the highly diluted solutions for a rapid matrix-assisted laser desorption/ionization (MALDI) or surface enhanced laser desorption ionization (SELDI) MS analysis [13–15]. Carbon materials, including graphene and carbon nanotube have also been used as a good matrix for analysis of small molecules by MALDI MS [16–21]. At the same time, the improvements in both ionization methods and MS instruments accelerate the analysis and characterization of carbon materials [22–24].

Mass spectroscopy continues to be one of the most important methods for the determination of the physical and chemical properties of carbon clusters. Carbon cluster cations of different sizes and different generation methods or sources have been widely studied [25–35]. Giant carbon clusters as large as C_{8000}^+ have been observed [29]. The methods of tandem MS, especially collisionally activated dissociation

Electronic supplementary material The online version of this article (doi:10.1007/s13361-011-0221-x) contains supplementary material, which is available to authorized users.

Correspondence to: Xianglei Kong; *e-mail:* kongxianglei@nankai.edu.cn, Yi Huang; *e-mail:* yihuang@nankai.edu.cn

Received: 5 May 2011
Revised: 21 July 2011
Accepted: 22 July 2011
Published online: 17 August 2011

(CAD) MS, have been used for different cluster ions including many endohedral fullerene ions in order to understand their structures and fragmentation behavior [26, 27, 36–39].

By contrast, there are fewer mass spectral studies of carbon cluster anions of large sizes with $n \geq 60$. McElvany et al. have reported even-numbered cluster anions from C_{60}^- to C_{124}^- by the method of methane negative ion chemical ionization [12]. The same group has also observed the large odd-numbered carbon clusters anions of C_{119}^-, C_{129}^- and C_{139}^- from the mass spectrum of a toluene extract of graphitic soot [3]. Sedo et al. have studied the laser desorption-ionization mass spectra of several kinds of materials, including graphite, glassy carbon, carbon nanotubes, synthetic diamond, and diamond-like thin layers [23]. Although carbon cluster ions from C_2 to C_{300} can be found in their positive ion products, only C_n^- ions with $n \leq 15$ can be identified in their negative mass spectra. Shibagaki et al. have investigated some carbon cluster ions by laser ablation of different polymers [24]. They found that negative clusters ions C_n^- with $n \geq 30$ are not observed from graphite, polyethylene, polypropylene, and polytetrafluoroethylene; however, for tetrafluoroethylene, large anions are observed up to $n = 120$. Interestingly, Maruyama observed even-numbered negative cluster ions of C_{120} - C_{160} by the laser ablation of a Ni - Co graphite disk while pure graphite never generates anion with such large sizes, showing that the metal atoms or clusters can strongly enhance the formation of large caged cluster anions [30]. Houska et al. have found weak signals of negatively charged cluster ions up to C_{200} or more in the laser desorption ionization process of nanodiamonds [29]. The largest carbon cluster anions previously observed may belong to the work of Jeon and coworkers [31]. With a chemical vapor deposition (CVD) process using gas mixtures of 1%–5% CH_4 and H_2, they observed clusters of ~3000 and ~18000 Da, which may contain ~250 and ~1500 carbon atoms if pure carbon atoms exist inside the clusters [31].

In the present work, the distributions of carbon cluster anions produced by laser ablation of graphene (G) and graphene oxide (GO) are analyzed. Carbon cluster anions as large as C_{500}^- have been observed. The effects of accumulation period and laser power on the distributions of anions are studied. CAD MS of selected anions also provides some interesting results.

Experimental

Instrumentation

All MS analyses were preformed with a 7.0 T Fourier transform ion cyclotron resonance mass spectrometer (FT ICR MS) instrument employing a MALDI source (Varian IonSpec ProMALDI). Mass spectra reported here were all measured in negative ion mode. Typically, ions produced by laser pulses are injected into an open-ended cylindrical Penning trap via an rf-only quadrupole ion guide. The open-ended cylindrical ICR cell contains two outer trapping plates. External and internal ion accumulation modes were combined in the experiments. With this mode, ions produced by six consecutive laser pulses were accumulated in the hexapole. In order to accomplish this, the hexapole DC potential and the hexapole exit lens are set to be 2 V and –10 V, respectively, during the accumulation time period. After the accumulation, the hexapole exit lens is gated so that ions can be transferred into the quadrupole guide. The DC potential of the trapping plate near the quadrupole was set to –15 V before the introduction of the ions into the cell. During the time period of ion transfer to the cell (0.8 to 12.5 ms used in the experiment , which is refer to as “accumulation period in the cell” hereinafter), the trapping plate is pulsed down to 0 V to allow the ions to enter into the ICR cell.

A 355 nm Nd: YAG laser (Orion, New Wave) was used to create ions. The frequency was set at 10 Hz, and the laser energy was set within the range of 28%–88% relative to the maximum energy of 4 mJ/pulse. All mass spectra were acquired over the *m/z* range of 220–5000. In the MS/MS study, the precursor ions of interest were selected by the stored waveform inverse Fourier transform (SWIFT) method [40]. Sustained off-resonance irradiation (SORI) [41] excitation was performed at amplitudes of 7.0–11.0 V ($V_{p\text{-}p}$) with a frequency offset of 1000 Hz relative to the precursor ion cyclotron frequency. During each 100 ms SORI event, the pressure in the ICR cell was raised to approximately 10^{-6} Torr by a brief pulse of nitrogen gas.

Sample Preparation

The sample of graphene oxide (GO) was prepared from natural graphite (average particle size of 20 μm, Qingdao Huarun Graphite Co., Ltd., Qingdao, China) by the modified Hummer method described in our previous work [42, 43].

The sample of graphene (G) was produced by reducing GO. GO was placed in a vacuum dessiccator, where a piece of filter paper saturated with the chemical reducing agent hydrazine (80% water solution) was placed for the first step of reduction. The reaction time was controlled for 24 h to generate the partially reduced graphene oxide. The partially reduced GO was then annealed in argon atmosphere at 1000°C to produce the samples of G [9].

Nanodiamonds with an average diameter of 100 nm were purchased from Beijing Grish Hi-Tech Corporation (Beijing, China). G, GO, and nanodiamonds were suspended in water at a concentration of 5 mg/mL and dispersed by sonication for 1 h prior to usage. A 1 μL of solution was then applied onto the MALDI target spots and dried at laboratory temperature before being placed into the source region of the FT ICR MS.

Results and Discussion

MS of G and GO

The mass spectrum of G by laser ablation is shown in Figure 1a. In the experiment, the laser energy was set at 48%

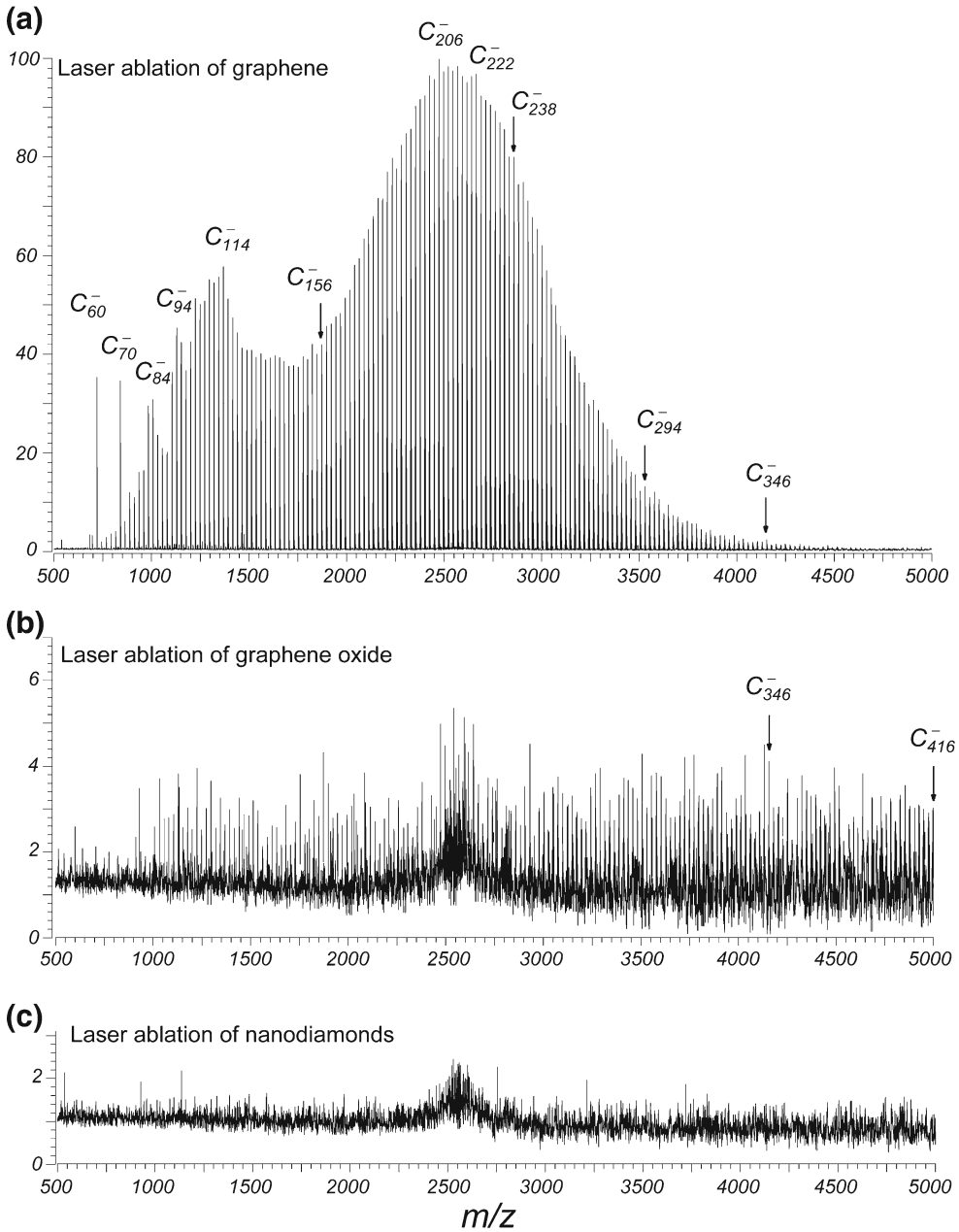

Figure 1. Mass spectra of negative carbon clusters produced by laser ablation of **(a)** G, **(b)** GO, and **(c)** nanodiamonds with an average size of 100 nm, obtained with a relative laser power of 48% and a cell accumulation time of 2.5 ms

and the accumulation time for ions in the cell was set as 2.5 ms. Strong signals of even-numbered carbon cluster anions were observed. The mass difference between consecutive carbon cluster ions is 24 *m/z* units. The peak intensities of C_{60}^- and C_{70}^- relative to their neighbors directly show their remarkable stabilities. There are at least three populations of carbon anions, which center at C_{84}^-,C_{114}^-, and C_{212}^-. The strong signals of C_{60}^-, C_{70}^-, and C_{84}^- are consistent with the negative mass spectrum of a toluene extract of graphitic soot reported by McElvany et al. [3]. However, the reported strong signals of C_{119}^-, C_{129}^- and C_{139}^- from the same spectrum are not observed here.

It is very interesting to see the formation of the carbon cluster anions with sizes larger than C_{200}. For comparison, the negative mass spectrum of nanodiamond (100 nm) was obtained here under the same conditions, and no cluster anions with size lager than $n \geq 80$ are observed (Figure 1c). Obviously, the formation of those cluster anions reflects the unique physical and chemical characteristics of graphene. Although the exact mechanism needs to be studied carefully by both experiments and theoretical calculations, a reasonable suggestion is that the formation can be mainly attributed to the unique electronic properties of graphene. This suggestion is supported by the experimental results for the

sample of GO. Under the same conditions, the negative mass spectrum of GO shows a wide distribution of carbon cluster anions from C_{90}^- to C_{500}^- (Figure 1b). Similar to the results for graphene, the even-numbered ions are separated by the C_2 unit. However, several differences can be easily identified by comparing Figure 1a and Figure 1b. First, signals of ions with *m/z* from 1000 to 4000 of GO are much weaker than those of graphene (about 1/30) and those ions are broad and well-distributed. Second, no magic cluster ions of C_{60}^- ,C_{70}^-, and C_{84}^- can be observed in the Figure 1b. Third, larger cluster anions with *m/z* greater than 4500 can be clearly observed in the mass spectrum of GO. By optimizing the detection parameters, the largest anions of C_{500}^- can be identified clearly (shown in the supporting materials). The first two points are more likely due to the electronic property differences between G and GO. The third point, however, may be attributed to their different size distribution or aggregation extent. It is also found that large anions up to C_{500}^- are observed in the mass spectrum of G, if the experimental conditions are optimized (data not shown here).

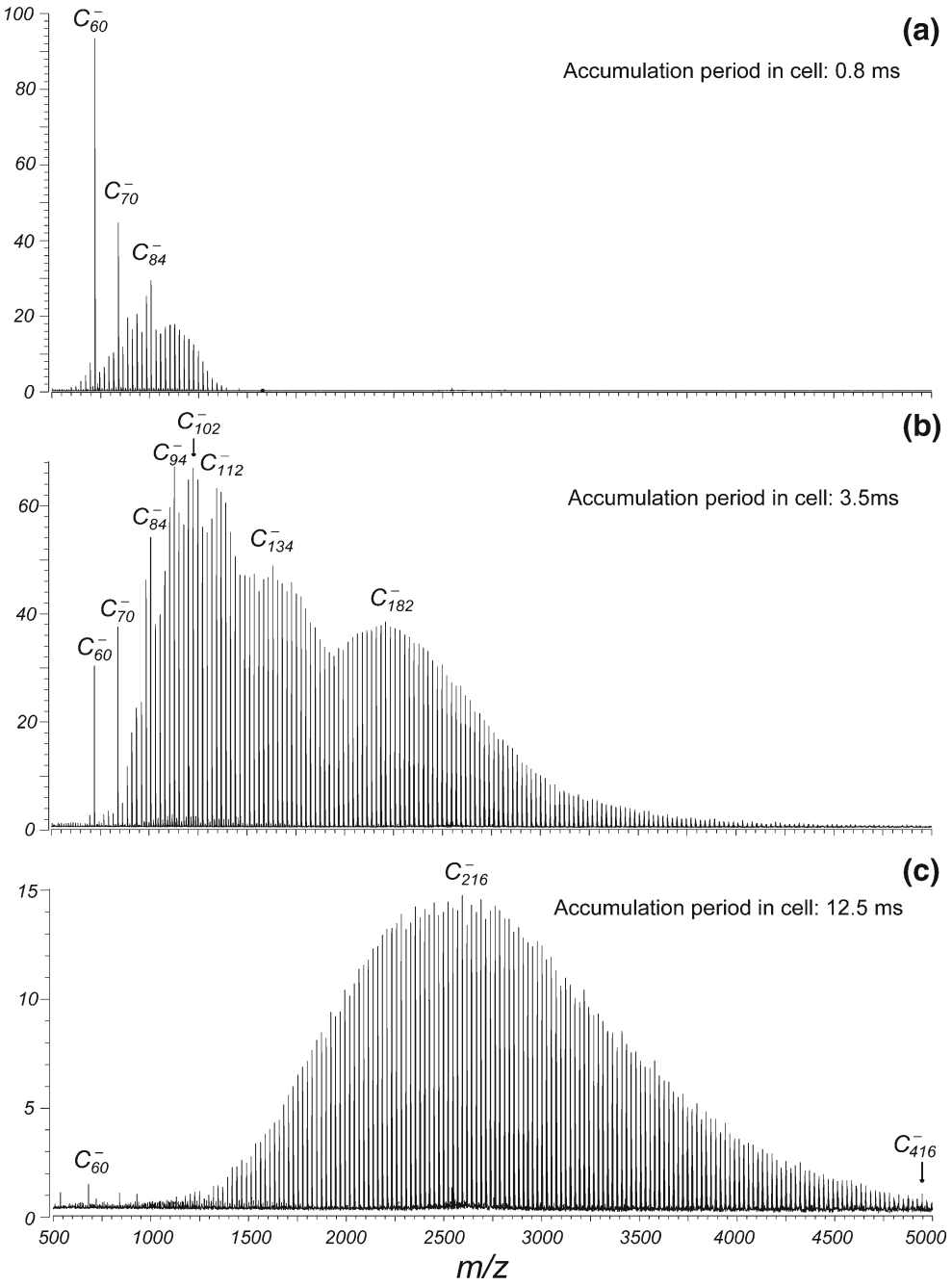

Figure 2. Mass spectra of negative carbon clusters produced by laser ablation of G under different accumulation periods of **(a)** 0.8 ms, **(b)** 3.5 ms, and **(c)** 12.5 ms. The laser power is set to 40%

Effects of Accumulation Period in the Cell and Laser Energy

It is observed that the accumulation period in the FT ICR cell can remarkably affect the observed cluster distribution. Figure 2 shows the mass spectra obtained with different accumulation periods under the same laser energy of 48%. For a very short accumulation period of 0.8 ms, the signals are located within the region of *m/z* from 500 to 1400, and the signals of C_{60}^- and C_{70}^- anions are dominant. When the accumulation period increases to 3.5 ms, three distributions can be observed, which are centered at C_{102}^-, C_{134}^- and C_{182}^-. Further increasing the period to 12.5 ms causes the population centered at C_{216}^- to have a broad distribution and lower intensity. The increase of the observed cluster sizes with the increasing accumulation periods can be understood by considering the transfer process of the ions. It is reasonable to suppose that the larger the cluster, the lower velocity it can acquire during the process of laser ablation. At the same time, large cluster ions have larger cross sections and, thus, can experience more collisions with residual gas. These facts indicate that the larger cluster ions require longer transfer times from the source region to the cell. Thus, a short opening time for the cell gate (short accumulation period) can cause the loss of the large cluster ions. From the results in Figure 2, it can be estimated that for the ions of C_{60}^- and C_{200}^-, their average axial velocities are ~2500 and ~350 m/s, respectively (considering the distance between the source and the cell is about 1.8 m). The high kinetic energy

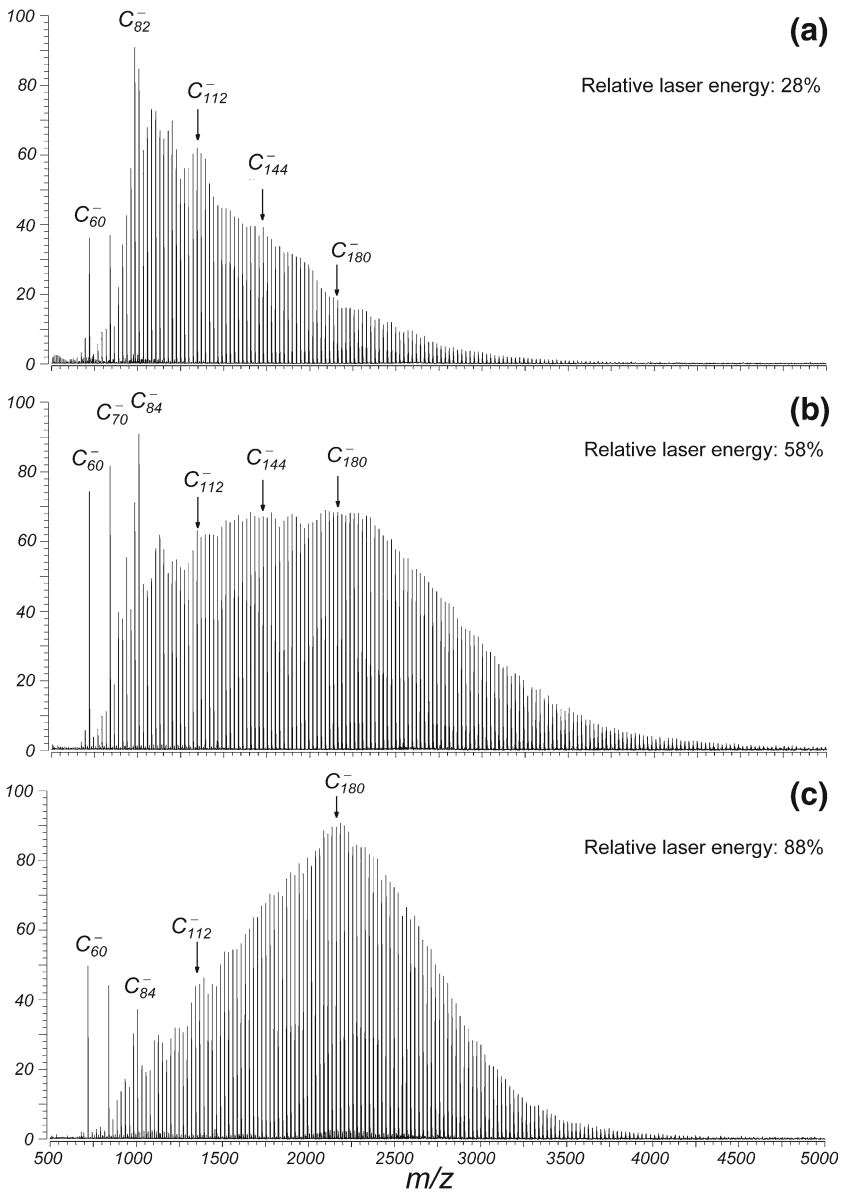

Figure 3. Mass spectra of negative carbon clusters produced by laser ablation of G under different laser powers at **(a)** 28%, **(b)** 58% and 88%, obtained with a cell accumulation time of 2 ms

of the ions can cause lower trapping efficiency and a decrease of ion signal, which is reflected in Figure 2c; the signals of small cluster ions were greatly reduced by increasing the accumulation time in the cell before the cool gas was added.

The distributions of cluster anions are also changed with different laser energies. Figure 3 shows three spectra obtained with laser energies at 28%, 58% and 88% respectively (the accumulation period is 2ms). As the laser energy increases from 28% to 58%, the intensity of medium and large anions (centered at C_{144}^- and C_{180}^-, respectively) increases rapidly while the intensity of small clusters centered at C_{94}^- decreases slightly. When the energy increases to 88%, both small and medium clusters decrease and the populations are sharpened.

However, a careful inspection of the weak ions generated among the strong even-numbered cluster anions can provide more details. It has been found that more ions with *m/z* from 300 to 900 can be produced with lower laser energy. Figure 4 shows the mass spectrum in low *m/z* regions at the laser energy of 28% (the strong signals of even-numbered, singly charged ions have been removed in order to clarify the spectrum.). Triply charged ions from C_{80}^{3-} to C_{224}^{3-} can be identified, and those ions are separated by a *m/z* difference of 8, indicating the clusters differ by a C_2 unit. Three distributions centered at C_{106}^{3-}, C_{152}^{3-} and C_{194}^{3-} can be found. Some cluster ions such as C_{84}^{3-} show higher stabilities than their neighbors. Interestingly, weaker signals of doubly charged ions from C_{70}^{2-} to C_{158}^{2-}(peaked at C_{106}^{2-}) can be observed in the same spectrum. Those ions are separated by a *m/z* unit of 24, indicating their clusters differ by a C_4 unit. This is verified by a close view of those triply charged ions, since some doubly charged ions have the same monoisotopic peaks as some triply charged ions, but their different isotopic distributions make them distinguishable.

As the laser energy increases, the signals of the triply charged ions decrease rapidly, while the doubly charged ions move to large *m/z* regions. Figure 5 shows the weak cluster ions at a laser power of 88%. No triply charged ions can be detected, and doubly charged ions with *m/z* values from 800 to 1500 can be identified. These doubly charged anions are separated by 12, instead of 24, mass units in Figure 5, and can be classified as two distributions centered at C_{176}^{2-} and C_{228}^{2-}. Interestingly, two populations of singly charged anions with odd number carbon atoms can be identified here, which center at C_{135}^- and C_{183}^-.

CAD MS Study

A variety of excitation methods have been used in conjunction with mass spectrometry and tandem mass spectrometry to reveal structural information of carbon cluster ions. Among the large carbon cluster anions, C_{60}^- is most commonly studied. It has been reported that the precursor ions of C_{60}^- can produce fragment ions of C_n^- with $n<20$, but the cross-sections are approximately 4 orders of magnitude smaller than those of C_{60}^+ [39, 44]. Interestingly, fragment ions of C_{2-30}^+ and even-numbered ions of C_{40-58}^+ were also observed from the CAD of C_{60}^- if the detection mode was set for positive ions. Here CAD experiments have been performed for C_{60}^- with N_2 as the collisional gas, and the lowest detectable *m/z* is set to be 220 in negative ion mode. No negative fragment ions with *m/z* larger than 220 have been detected by the CAD process of C_{60}^-, which is consistent with previous results. This result seems is expected due to the ultra stability of this magic cluster. It is also expected that the non-magic larger carbon cluster anions can readily produce fragment ions by the ejection of C_2 units (or other units) through the CAD

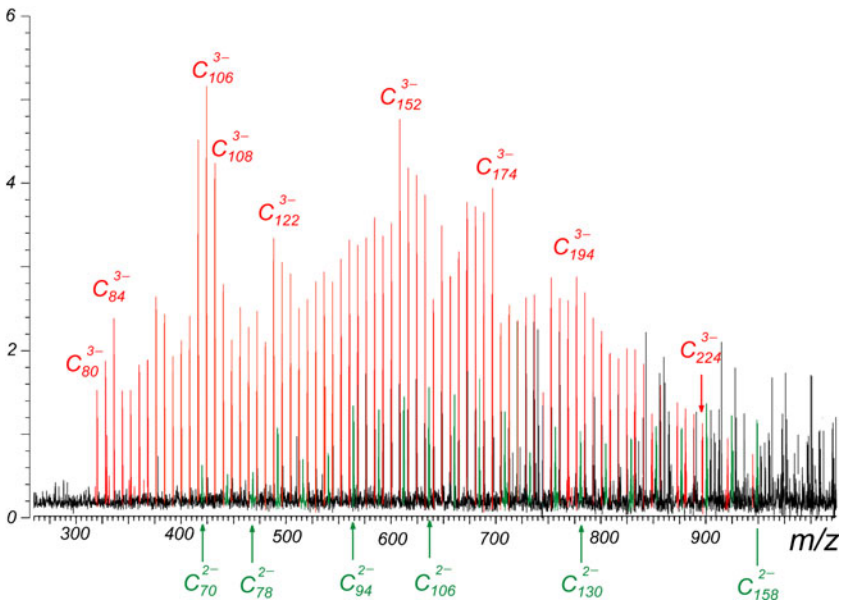

Figure 4. Mass spectra of negative carbon clusters in the low *m/z* region produced by laser ablation of G with a relative laser power of 28%. The strong signals of singly charged anions are removed in order to clarify the spectrum

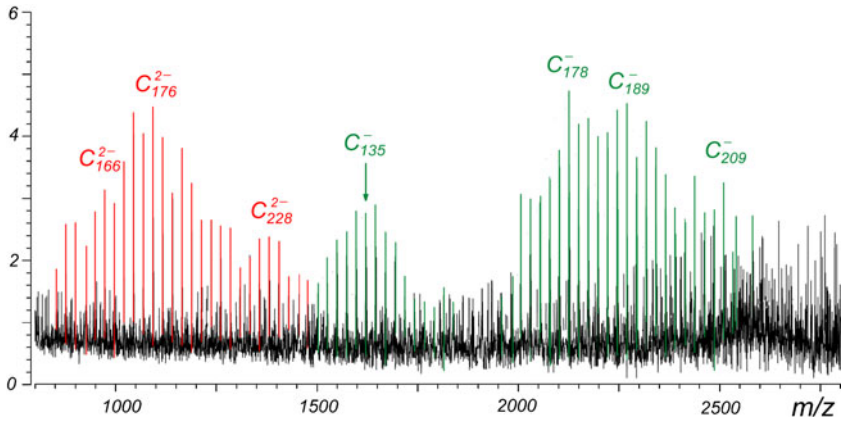

Figure 5. Weak signals of doubly charged anions and odd-numbered anions observed in the mass spectrum of negative carbon clusters produced by laser ablation of G with a power of 88%. The strong signals of singly charged anions are removed in order to clarify the spectrum

process. In order to observe those presumed dissociation processes, eight different anions of C_{84}^-, C_{114}^-, C_{176}^-, C_{180}^-, C_{206}^-, C_{228}^-, C_{254}^- and C_{258}^- are selected and studied by CAD. The source conditions are the same as those in Figure 1a, from which it can be deduced directly that the anions of C_{84}^-, C_{114}^- and C_{206}^- may be more stable than other typical non-magic anions: C_{176}^-, C_{180}^-, C_{228}^-, C_{254}^- and C_{258}^- . However, the CAD results are surprising. No negative fragment ions with *m/z* larger than 220 can be observed from the collision of those anions except the ion of C_{228}^-, although the stabilities of those anions are similar (a $V_{p\text{-}p}$ of 10.5 V in SORI CAD process can cause more than 90% precursor ion disappearance in their mass spectra). The CAD MS of C_{228}^- shows two fragment ions of C_{224}^- and C_{222}^- (see Supporting Information), and with increasing collision energy, the precursor ions decreased without the appearance of other fragment ions. The fragment ions of C_{222}^- are not seen as product ions from C_{224}^-, since the CAD of the isolated C_{224}^- does not produce any fragments.

Why is the anion of C_{228}^- so special and how stable are the other cluster anions? In order to better understand this issue, the even-numbered anions in a small region from C_{200}^- to C_{240}^- have been isolated and studied by CAD. Among these 21 even-numbered cluster ions, 14 kinds of ions show no fragment ions while seven kinds of ions form different fragment ions by loss of the units of C_2, C_4, C_6, or C_8. Those results are shown in Figure 6. For example, the C_{234}^- ion can dissociate to C_{228}^- mainly by losing the C_6 unit, and also can dissociate to C_{226}^- by losing the C_8 unit (see Supporting Information). The anions of C_{220}^-, C_{216}^- and C_{212}^- are all characterized by the unique process of losing the C_4 unit while C_{222}^- can lose a C_6 unit solely.

The CAD results of those carbon cluster anions seem very confusing. For cluster ions of atoms and molecules, it is always expected and proven that the change of their structures and

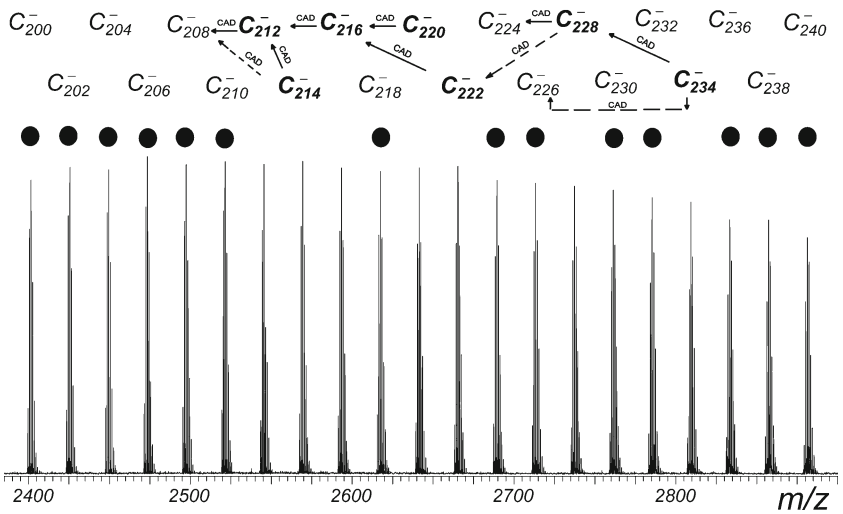

Figure 6. CAD pathways of selected even-numbered anions from C_{200}^- to C_{240}^-. The mass spectrum (a portion of Figure 1a) shows very similar abundances for those cluster ions. For the anions marked by solid circles, no negative fragment ions larger than C_{20}^- can be observed in corresponding CAD mass spectra. The dissociation pathways for other anions are marked by solid arrows (primary pathways) and dashed arrows (secondary pathways)

dissociation pathways can occur progressively as their sizes increase. There may be exceptions for cluster ions with extra stabilities or very high symmetry, which can be reflected in their mass spectra as magic clusters. But for the case here, no cluster ion in Figure 6 is substantially more stable than others.

Why do these seven kinds of ions behave differently from the others? The structural difference makes us recall the dangling bonds previously suggested for small size cluster ions [2]. Their individual behaviors in the CAD process may be explained by the different numbers of possible dangling bonds. In the process of forming anion clusters by laser ablation, the pentagon rule may be violated. Thus, it is possible that some cluster anions can form open structures with some dangling bonds, which can be easily ejected during collision; however, most of the ions still have closed fullerene structures. Determination of clear answers and the exact structures of those cluster anions require a thorough experimental and theoretical study.

Conclusions

Unlike other carbon materials, graphene can produce carbon cluster anions with sizes up to C_{500}^- readily by the process of laser ablation at the wavelength of 355 nm. Wide distributions of anions from C_{90}^- to C_{500}^- can also be observed by the laser ablation of GO, but the signals are much weaker. The even-numbered cluster anions generated from G show several distributions, which can be readily controlled by changing the accumulation periods in an FT-ICR cell and laser energies. Weak signals of triply charged cluster anions from C_{80}^{3-} to C_{224}^{3-} and doubly charged anions from C_{70}^{2-} to C_{158}^{2-} can be observed with lower laser energy, while odd-numbered singly charged anions from C_{119}^- to C_{209}^- can be observed at higher laser energy.

Some cluster anions were studied by collisional activation by N_2 gas. Although no negatively charged fragments larger than C_{20}^- can be observed for most of those cluster ions, some cluster anions can form fragment ions by loss C_2, C_4, C_6, or C_8 units. Since those ions have similar stabilities as their neighbors, the origin of their different behaviors requires further study.

Acknowledgments

The authors gratefully acknowledge financial support from the National Natural Science Foundation of China (no. 21052001, 50902073) and Ministry of Education (no. 708020).

References

1. Kroto, H.W., Heath, J.R., O'Brien, S.C., Curl, R.F., Smalley, R.E.: C_{60}: buckminsterfullerene. *Nature* **318**, 162–163 (1985)
2. Smalley, R.E.: Self-assembly of the fullerenes. *Acc. Chem. Res* **25**, 98–105 (1992)
3. McElvany, S.W., Callahan, J.H., Ross, M.M., Lamb, L.D., Huffman, D. R.: Large odd-number carbon clusters from fullerene-ozone reactions. *Science* **260**, 1632–1634 (1993)
4. Lijima, S.: Helical microtubules of graphitic carbon. *Nature* **354**, 56–58 (1991)
5. Ajayan, P.M.: Nanotubes form carbon. *Chem. Rev* **99**, 1787–1799 (1999)
6. Novoselov, K.S., Geim, A.K., Morozov, S.V., Jiang, D., Zhang, Y., Dubonos, S.V., Grigorieva, I.V., Firsov, A.A.: Electric field effect in atomically thin carbon films. *Science* **306**, 666–669 (2004)
7. Geim, A.K., Novoselov, K.S.: The rise of graphene. *Nat. Mater* **6**, 183–191 (2007)
8. Li, X., Wang, X., Zhang, L., Lee, S., Dai, H.: Chemically Derived, Ultrasmooth graphene nanoribbon semiconductors. *Science* **319**, 1229–1232 (2008)
9. Castro Neto, A.H., Guinea, F., Peres, N.M.R., Novoselov, K.S., Geim, A.K.: The electronic properties of graphene. *Rev. Mod. Phys* **81**, 109–162 (2009)
10. Wang, Y., Huang, Y., Song, Y., Zhang, X., Ma, Y., Liang, J., Cheng, Y.: room-temperature ferromagnetism of grapheme. *Nano Lett* **9**, 220–224 (2009)
11. Abanin, D.A., Morozov, S.V., Ponomarenko, L.A., Gorbachev, R.V., Mayorov, A.S., Katsnelson, M.I., Watanabe, K., Taniguchi, T., Novoselov, K.S., Levitov, L.S.: Giant nonlocality near the Dirac point in grapheme. *Science* **332**, 328–330 (2011)
12. McElvany, S.W., Ross, M.M.: Mass spectrometry and fullerenes. *J. Am. Soc. Mass Spectrom* **3**, 268–280 (1992)
13. Kong, X.L., Huang, L.C.L., Hsu, C.M., Chen, W.H., Han, C.C., Chang, H.C.: High-Affinity Capture of Proteins by Diamond Nanoparticles for Mass Spectrometric Analysis. *Anal. Chem* **77**, 259–265 (2005)
14. Kong, X., Huang, L.C.L., Liau, S.C.V., Han, C.C., Chang, H.C.: Polylysine-coated diamond nanocrystals for MALDI-TOF mass analysis of DNA oligonucleotides. *Anal. Chem* **77**, 4273–4277 (2005)
15. Tang, L.A.L., Wang, J., Loh, K.P.: Graphene-based SELDI probe with ultrahigh extraction and sensitivity for DNA Oligomer. *J. Am. Chem. Soc* **132**, 10976–10977 (2010)
16. Xu, X.Y., Li, Y.F., Zou, H.F., Qiu, J.S., Guo, Z., Guo, B.C.: Carbon nanotubes as assisted matrix for laser desorption/Ionization time-of-flight mass spectrometry. *Anal. Chem* **75**, 6191–6195 (2003)
17. Ren, S.F., Guo, Y.L.: Oxidized carbon nanotubes as matrix for matrix-assisted laser desorption/ionization time-of-flight mass spectrometric analysis of biomolecules. *Rapid Commun. Mass Spectrom* **18**, 1455–1458 (2005)
18. Pan, C.S., Xu, X.Y., Hu, L.G., Su, X.Y., Ou, J.J., Zou, H.F., Guo, Z., Zhang, Y., Guo, B.C.: Using oxidized carbon nanotubes as matrix for analysis of small molecules by MALDI-TOF MS. *J. Am. Soc. Mass Spectrom* **16**, 883–892 (2005)
19. Cha, S., Yeung, E.S.: Colloidal graphite-assisted laser desorption/ionization mass spectrometry and MS^n of small molecules. 1. Imaging of cerebrosides directly from rat brain tissue. *Anal. Chem* **79**, 2373–2385 (2007)
20. Dong, X., Cheng, J., Li, J., Wang, Y.: Graphene as a novel matrix for the analysis of small molecules by MALDI-TOF MS. *Anal. Chem.* **82**, 6208–6214 (2010)
21. Lu, M., Lai, Y., Chen, G., Cai, Z.: Matrix Interference-Free Method for the Analysis of Small Molecules by Using Negative Ion Laser Desorption/Ionization on Graphene Flakes. *Anal. Chem* **83**, 3161–3169 (2011)
22. Greenwood, P.F., Strachen, M.G., EI-Nakat, H.J., Willett, G.D., Wilson, M.A., Attalla, M.I.: Laser ablation Fourier transform mass spectrometric investigation of coals and model materials. *FUEL* **69**, 257–260 (1990)
23. Sedo, O., Alberti, M., Janca, J., Havel, J.: Laser desorption-ionization time of flight spectrometry of various carbon materials. *Carbon* **44**, 840–847 (2006)
24. Shibagaki, K., Takada, N., Sasaki, K., Kadota, K.: Synthetic characteristics of large carbon cluster ions by laser ablation of polymers in vacuum. *J. Appl. Phys* **93**, 655–661 (2003)
25. Clemmer, D.E., Jarrold, M.F.: Metal-containing carbon clusters: structures, isomerization and formation of NbCn+clusters. *J. Am. Chem. Soc.* **117**, 8841–8850 (1995)
26. Van Orden, A., Saykally, R.J.: Small Carbon Clusters: Spectroscopy, Structure, and Energetics. *Chem. Rev.* **98**, 2313–2358 (1998)
27. Lifshitz, C.: Carbon clusters. *Int. J. Mass Spectrom.* **200**, 423–442 (2000)
28. Belau, L., Wheeler, S.E., Ticknor, B.W., Ahmed, M., Leone, S.R., Allen, W.D., Schaefer, H.F., Duncan, M.A.: Ionization thresholds of small carbon clusters: tunable VUV experiments and theory. *J. Am. Chem. Soc.* **129**, 10229–10243 (2007)

29. Houska, J., Panyala, N.R., Pena-Mendez, E.M., Havel, J.: Mass spectrometry of nanodiamonds. *Rapid Commun. Mass Spectrom.* **23**, 1125–1131 (2009)
30. Maruyama, S.: FT-ICR reaction experiments and molecular dynamics simulations of precursor clusters for SWNTS. *Perspectives of fullerene nanotechnology.* Part III. pp. 131–142 (2002)
31. Jeon, I.D., Park, C.J., Kim, D.Y., Hwang, N.W.: Effect of methane concentration on size of charged clusters in the hot filament diamond CVD proves. *J. Crystal Growth* **213**, 6–14 (2001)
32. Campbell, E.E.B., Ulmer, G., Hasselberger, B., Busmann, H.-G., Hertel, I.V.: An intense, simple carbon cluster source. *J. Chem. Phys.* **93**, 6900–6907 (1990)
33. Campbell, E.E.B., Ulmer, G., Hertel, I.V.: Delayed ionization of C_{60} and C_{70}. *Phys. Rev. Lett.* **67**, 1986–1988 (1991)
34. Campbell, E.E.B., Ulmer, G., Hertel, I.V.: Thermionic emission from the fullerenes. *Z. Phys. D* **24**, 81–85 (1992)
35. Zettergren, H., Johansson, H.A.B., Schmidt, H.T., Jensen, J., Hvelplund, P., Tomita, S., Wang, Y., Martín, F., Alcamí, M., Manil, B., Maunoury, L., Huber, B.A., Cederquist, H.: Magic and hot giant fullerenes formed inside ion irradiated weakly bound C_{60} Clusters. *J. Chem. Phys.* **133**, 104301 (2010)
36. Brink, C., Hveplund, P., Shen, H., Jimenez-Vazquez, H.A., Cross, R.J., Saunders, M.: Collisional fragmentation of $Ar@C_{60}$. *Chem. Phys. Lett.* **286**, 28–34 (1998)
37. Deng, R., Echt, O.: Hyperthermal collisions of atomic clusters and fullerenes. *Int. J. Mass Spectrom.* **233**, 1–12 (2004)
38. Cordero, M.M., Cornish, T.J., Cotter, R.J.: Matrix-Assisted Laser Desorption/Ionization Tandem Reflectron Time-of-Flight Mass Spectrometry of Fullerenes. *J. Am. Soc. Mass Spectrom.* **7**, 590–597 (1996)
39. Larsen, M.C., Hvelplund, P., Larsson, M.O., Shen, H.: Fragmentation of fast positive and negative C_{60} ions in collisions with rare gas atoms. *Eur. Phys. J. D.* **5**, 283–289 (1999)
40. Cody, R.B., Hein, R.E., Goodman, S.D., Marshall, A.G.: Stored waveform inverse Fourier transform excitation for obtaining increased parent ion selectivity in collisionally activated dissociation: Preliminary results. *Rapid Commun. Mass Spectrom.* **1**, 99–102 (1987)
41. Gauthier, J.W., Trautman, T.R., Jacobson, D.B.: Sustained off-resonance irradiation for collision-activated dissociation involving Fourier-transform mass-spectrometry-collision-activated dissociation technique that emulates infrared multiphoton dissociation. *Anal. Chim. Acta* **246**, 211–225 (1991)
42. Becerril, H.A., Mao, J., Liu, Z., Stoltenberg, R.M., Bao, Z., Chen, Y.: Evaluation of solution-processed reduced graphene oxide films as transparent conductors. *ACS Nano* **2**, 463–470 (2008)
43. Liang, J., Huang, Y., Zhang, L., Wang, Y., Ma, Y., Guo, T., Chen, Y.: Molecular-level dispersion of graphene into poly(vinyl alcohol), and effective reinforcement of their nanocomposites. *Adv. Funct. Mater.* **19**, 2297–2302 (2009)
44. Mathur, D., Brink, C., Hveplund, P., Jensen, N., Yu, D.H.: Collision-induced dissociation of C_{60}^-: effect of energy-coupling process on the dissociation dynamics. *Rapid Commun. Mass Spectrom.* **9**, 114–118 (1995)